ACTA MONTANA 1992
Series A, No. 3(89), 165-188

DIFFERENCES BETWEEN EARTHQUAKES AND EXPLOSION SOURCES IN NORTH WESTERN BOHEMIA

Václav Bucha

Institute of Geotechnics, Czechoslovak Academy of Sciences,
V Holešovičkách 41, 182 09 Prague, Czechoslovakia.

Abstract: The aim of the paper is to determine features of seismograms of earthquakes, refraction explosions and quarry blasts, which could be utilized for an automatic seismic discrimination in North Western Bohemia.

Key words: earthquakes, explosion sources, discrimination

1. INTRODUCTION

A great effort is devoted to automatic discrimination of seismic events. Many algorithms can be used in certain regions with various reliability. An important task is to find characteristic features of seismograms for discrimination. The paper summarizes results, which were achieved by the analysis of seismograms of earthquakes, refraction explosions and quarry blasts in North Western Bohemia. Amplitude, frequency and polarization analysis were used to determine distinguishable properties of earthquakes and explosion sources.

2. DIFFERENCES BETWEEN EARTHQUAKES AND EXPLOSION SOURCES

The mechanism of the source of tectonic earthquake is derived from the common equations for elastic anizotropic homogeneous medium (Aki and Richards, 1980). The displacement field $u_n(\vec{x},t)$ at a point $\vec{x}$ of the volume V with the surface S, and at a time t, in presumption of validity of the Hooke law and of the continuum equation in the whole volume V (Fig.1), is described by the

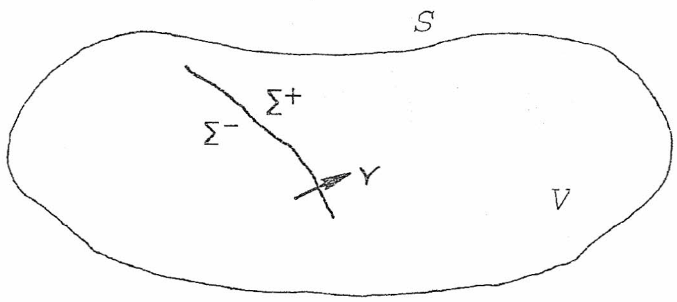

Fig. 1. Idealized model of the fault double-sided surface Σ in the volume V (Aki and Richards, 1980)

representation theorem

$$
\begin{aligned}
u_n(\vec{x},t) = & \int_{-\infty}^{\infty} d\tau \iiint_V f_p(\vec{\eta},\tau) G_{np}(\vec{x},t-\tau;\vec{\eta},0)\, dV(\vec{\eta}) \\
& + \int_{-\infty}^{\infty} d\tau \iint_\Sigma \{[u_i(\vec{\xi},\tau) c_{ijpq}\, \nu_j \frac{\delta}{\delta \xi_q} G_{np}(\vec{x},t-\tau;\vec{\xi},0)] \\
& - [G_{np}(\vec{x},t-\tau;\vec{\xi},0) T_p(\vec{u}(\vec{\xi},\tau),\vec{\nu})]\} d\Sigma \ , \qquad (1)
\end{aligned}
$$

where f_p is the body force, G_{np} is the Green function, T_p is the tension on the surface Σ, c_{ijpq} are elastic coefficients , $\vec{\nu}$ is the normal with respect to the surface Σ, $\vec{\eta}$ refers to a point of the volume V a $\vec{\xi}$ refers to a point of the surface Σ. The outer boundary of the volume V is the surface S and the inner boundary is the fault double-sided surface Σ^+, Σ^-, the surface S is free and there are no tensions T_p, the Green function G of fault surface Σ fulfils homogeneous boundary condition independently on a time (G or $\frac{\delta}{\delta t} G$ is zero at the fault surface Σ). The volume integral in the equation (1) expresses the displacement field caused by volume forces and another two members represent contributions that arise from the tension and the displacement on the fault.

Sharpe (1942) has chosen to state the problem of the generation of elastic waves by explosion pressures as follows: Given a spherical cavity of radius a within a homogeneous, ideally elastic, infinite medium of density ρ and compressional wave velocity v ; to find the elastic wave motion which results from application of an arbitrary

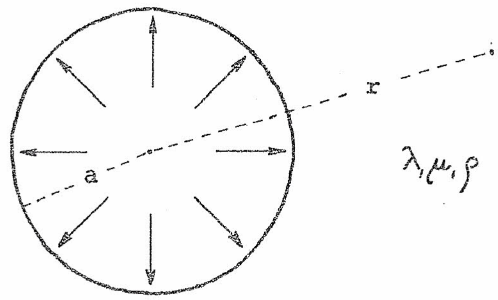

Fig. 2. Illustration of the idealized model of the problem of the generation of elastic waves by explosion pressures (Sharpe, 1942).

pressure $p(t)$ to the interior surface of the cavity (Fig. 2). The displacement at distances more than a few times the radius of the cavity is represented quite adequately by the simple expression

$$u = \frac{a^2 p_0}{2\sqrt{2}\mu r} e^{-\omega\tau/\sqrt{2}} \sin \omega\tau \qquad \text{for } \tau \geq 0 \qquad (2)$$

$$u = 0 \qquad \text{for } \tau < 0 \text{ ,}$$

where p_0 is a constant representing the initial, and highest, pressure attained, $\omega \equiv 2\sqrt{2}v/3a$, $\tau = t-(r-a)/v$, r is the distance.

Ripple-fired quarry blasts, events that involve a number of subexplosions closely grouped in space and time, are commonly used in quarries (Hedlin et al., 1990). The dimensions of quarry blasts are of the order of tenths of meters. Using $u(t)$ as the seismic signal from a single shot and assuming a constant time delay δ_t between each shot or set of simultaneous shots (e.g., a row of shots), the signal $s(t)$ from the ripple-fired blast is the sum of all N shots or rows (Smith, 1989)

$$s(t) = \sum_{m=0}^{N-1} h(m\delta_t)u(t-m\delta_t) \text{ ,} \qquad (3)$$

where $h(m\delta_t)$ represents the number of charges at time $m\delta_t$ from the initiation of the blast. If time delays between shots are not uniform, we can represent this as a continuous integral

$$s(t) = \int_{\tau=0}^{t_N} h(\tau)u(t-\tau)d\tau \ , \tag{4}$$

where t_N is the total duration of the blast and $h(\tau)$ describes either the number of charges exploding at a specific time τ or the total size of charges initiated at time τ.

The criteria that have been used by various authors (Hussein, 1989, Deneva et al., 1988, Dysart et al., 1990, Hedlin et al., 1989,1990, Smith, 1989, Su et al., 1991) for discrimination between earthquakes and explosion sources are the following:

1. *Direction of P wave arrival*

The P waves generated by explosions should be compression everywhere, but the P waves generated by earthquakes should be compression in two quadrants and dilatation in two remaining quadrants.

2. *Generation of S waves*

An explosion generates mainly the P waves, with S waves completely vanishing or being very weak. The earthquakes generate both S and P waves, the S waves being several times stronger than P waves.

3. *Surface waves*

The explosions are situated close to the Earth's surface, so they should generate stronger surface waves than the earthquakes. However, the surface waves are better generated by low frequency S waves than by high frequency P waves.

4. *Predominant frequencies*

The characteristic dimension of the rupture surface is usually considerably larger than the characteristic dimension of the volume of explosions. The predominant frequencies should be lower for earthquakes than for explosions.

5. *Oscillation of amplitude spectra*

Quarry blasts consist of a number of subexplosions closely grouped in space and time. They produce signals that are superposition of the wavefields produced by each of the subevents and that can interfere.

6. *High frequency energy*

There is a lack of energy in high frequencies for quarry blasts as compared to earthquakes.

3. SEISMIC DATA

The eight processed earthquakes occurred in the Kraslice swarm region and one event was near Cínovec (Fig. 3). Table I contains the fundamental information about observed earthquakes. Refraction explosions in boreholes for the structural study of Western Bohemia were performed by Geofyzika Brno. Four explosions measured also by the Institute of Geotechnics and the Geophysical Institute were chosen in this paper (Fig. 3, Tables II, III, IV). Quarry blasts in boreholes or galleries from 15 different quarries were selected for further analysis (Fig. 3, Tables V, VI).

The processed data were measured by seismic stations of the Institute of Geotechnics: Hora sv. Kateřiny (HSK), Křížatky (KRI), Pyšná (PYS), Jezerka (JEZ) and some temporary measurement points which measured refraction explosions (Fig. 3, Tables III, VII). The stations HSK, KRI, PYS, JEZ recorded expected induced seismic events near open-pit mines in North Bohemian Coal Basin (Bucha and Jíra, 1992). The data from seismic station Nový Kostel (NKC) of the Geophysical Institute, that lies in the Kraslice swarm region, were also used. All the data were measured by digital equipments with the sampling frequency in the range 125 to 250 Hz.

Table I. Processed earthquakes

	time (UTC) y m d h m	station	coordinates ϕ [°]	λ [°]	ΔNKC [km]	ΔHSK [km]	M_L HSK
1	89.03.22 00:03	HSK	50.74	13.81	-	30	0.90
2	91.03.24 05:05	HSK,NKC	50.30	12.23	17	92	2.22
3	91.03.24 09:38	HSK,NKC	50.28	12.22	17	93	1.65
4	91.03.24 14:33	HSK,NKC	50.29	12.22	17	93	2.62
5	91.03.24 15:01	HSK,NKC	50.29	12.22	17	92	1.80
6	91.03.24 15:41	HSK,NKC	50.29	12.22	17	93	1.68
7	91.03.25 14:54	HSK,NKC	50.30	12.22	17	92	2.62
8	91.04.22 22:25	HSK,NKC	50.36	12.14	26	96	1.46
9	91.05.19 03:22	HSK,NKC	50.36	12.37	15	79	2.41

Table II. Refraction explosions

time (UTC) y m d h m	shot point	charge [kg]	coordinates ϕ [°]	λ [°]	H [m]
91.07.03 14:00	C1-Libá	49	50.129	12.216	561
91.07.03 15:00	C2-Skalná	49	50.182	12.346	519
91.07.03 16:00	C3-Čirá	70	50.286	12.464	623
91.07.03 17:00	C4-Šindelová	140	50.352	12.588	853

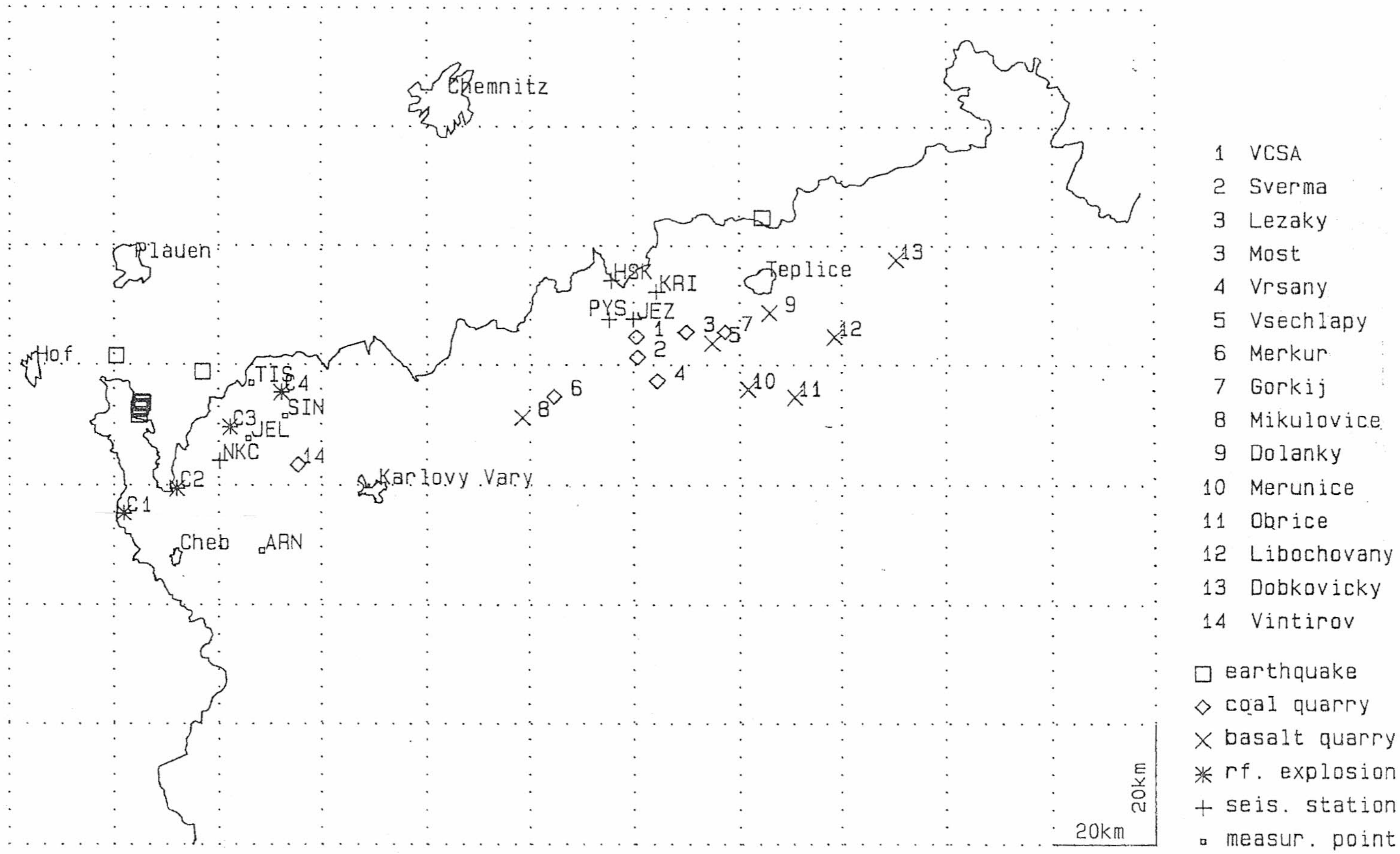

Fig. 3. Map of North Western Bohemia showing earthquakes, quarries, refraction explosions, seismic stations and measurement points.

Table III. Measurement points

station	*coordinates*		
	ϕ *[°]*	λ *[°]*	*H [m]*
Arnoltov-ARN	50.112	12.595	588
Jelení vrch-JEL	50.274	12.519	677
Tisová-TIS	50.357	12.507	638
Šindelová-SIN	50.318	12.606	616

Table IV. Refraction measurements

time (UTC) *y m d h m*	*station*	ΔARN *[km]*	ΔJEL *[km]*	ΔTIS *[km]*	ΔSIN *[km]*	ΔNKC *[km]*	M_L NKC
91.07.03 14:00	TIS	–	–	33	–	–	–
91.07.03 15:00	ARN, TIS,SIN,NKC	19	–	23	24	9	0.19
91.07.03 16:00	JEL,TIS, NKC	–	4	9	–	6	0.46
91.07.03 17:00	ARN,JEL,TIS, NKC	27	10	6	–	17	0.36

Table V. Quarries

quarry	*coordinates*		ΔHSK *[km]*	ΔNKC *[km]*	ΔKRI *[km]*	ΔPYS *[km]*	ΔJEZ *[km]*	*mate-rial*
	ϕ *[°]*	λ *[°]*						
VČSA	50.53	13.52	10	83	8	6	3	coal
Šverma	50.50	13.53	14	82	12	8	6	coal
Ležáky	50.55	13.65	17	92	–	–	–	coal
Most	50.55	13.65	17	92	–	–	–	coal
Vršany	50.47	13.59	19	85	–	–	–	coal
Všechlapy	50.54	13.72	22	96	–	–	–	basalt
Merkur	50.42	13.32	22	65	–	–	–	coal
Gorkij	50.56	13.75	23	99	–	–	–	coal
Mikulovice	50.38	13.24	29	58	–	–	–	basalt
Dolánky	50.60	13.86	30	108	–	–	–	basalt
Měrunice	50.48	13.83	35	105	–	–	–	basalt
Obřice	50.48	13.96	39	110	–	–	–	basalt
Libochovany	50.58	14.05	44	120	–	–	–	basalt
Dobkovičky	50.71	14.19	55	134	–	–	–	basalt
Vintířov	50.25	12.66	68	15	–	–	–	coal

Table VI. Quarry blasts

	time (UTC) *y m d h m*	*station*	*quarry*	*total charge [kg]*	*max. charge per subexp. [kg]*	*number of subexp-losions*	M_L *HSK*
1	88.02.11 13:04	HSK	Ležáky	1800	180	10	1.18
2	88.03.14 10:32	HSK	Ležáky	2000	200	10	1.22
3	88.03.14 10:35	HSK	Ležáky	2000	200	10	1.37
4	88.03.17 10:07	HSK	Ležáky	1400	140	10	0.92
5	88.05.02 10:30	HSK	Ležáky	1000	55	18	0.99
6	88.05.19 09:49	HSK	Most	1842	184	10	0.63
7	88.05.19 12:20	HSK	Most	1842	184	10	0.61
8	88.06.21 08:25	HSK	Most	1000	100	10	0.94
9	88.06.23 09:37	HSK	Most	700	70	10	1.13
10	88.09.29 10:29	HSK	Všechlapy	2270	567	4	0.79
11	88.11.01 13:57	HSK	VČSA	7525	452	17	1.86
12	89.01.05 09:00	HSK	Mikulovice	10420	2434	5	1.56
13	89.06.20 11:24	HSK	Vintířov	3942	365	11	1.47
14	90.04.09 12:06	HSK,NKC	Gorkij	7104	470	19	0.89
15	90.04.11 10:59	HSK	Gorkij	3796	241	16	0.74
16	90.04.11 12:34	HSK,NKC	Vršany	3880	388	10	0.91
17	90.04.12 08:54	HSK,NKC	Merkur	3955	209	19	1.01
18	90.04.13 07:25	HSK	Most	680	68	10	0.41
19	90.04.13 08:50	HSK	Merkur	3327	223	19	1.05
20	90.04.13 12:19	HSK	Vršany	3035	303	10	0.58
21	90.04.14 10:24	HSK,NKC	Gorkij	3048	135	23	0.67
22	90.04.15 10:41	HSK	Vršany	2910	291	10	0.55
23	90.04.17 11:05	HSK,NKC	Vintířov	3289	286	12	0.89
24	90.04.18 07:34	HSK,NKC	Merkur	4330	413	19	1.24
25	90.04.18 12:05	HSK	Gorkij	5590	483	19	0.49
26	90.04.20 08:12	HSK	Šverma	725	181	4	0.85
27	90.04.20 08:44	HSK	Merkur	1451	112	13	0.73
28	90.04.20 09:30	HSK,NKC	Gorkij	2511	202	15	0.89
29	90.04.20 11:00	HSK,NKC	Měrunice	5253	2941	3	1.05
30	90.04.22 07:34	HSK	Šverma	504	126	4	0.61
31	90.04.23 11:48	HSK	Vršany	2430	243	10	0.44
32	90.04.24 12:52	HSK	Vršany	1945	194	10	0.56
33	90.04.25 07:41	HSK,NKC	Merkur	3970	401	19	1.29
34	90.04.28 11:00	HSK	Gorkij	4520	301	16	0.64
35	90.04.29 11:14	HSK	Gorkij	6685	361	19	0.62
36	90.04.30 11:33	HSK,NKC	Vršany	5000	500	10	0.84
37	90.05.03 11:03	HSK	Dolánky	2722	340	8	0.77
38	90.05.03 13:04	HSK,NKC	VČSA	5365	452	14	1.76
39	90.05.04 12:32	HSK	VČSA	2197	151	15	1.44
40	90.05.07 11:54	HSK	VČSA	4286	301	16	1.55
41	90.05.08 09:41	HSK,NKC	VČSA	5930	301	20	1.63
42	90.05.10 10:08	HSK,NKC	VČSA	3462	301	12	1.72
43	90.05.13 12:20	HSK	VČSA	3866	301	13	1.59
44	90.05.15 07:21	HSK	Všechlapy	1651	659	3	0.59
45	90.05.16 09:59	HSK,NKC	Obřice	4720	1700	4	0.64
46	90.05.17 08:19	HSK	Dobkovičky	19400	4990	4	1.63
47	90.05.18 11:54	HSK,NKC	Šverma	2410	482	5	1.10
48	90.05.22 13:24	HSK,NKC	Šverma	3747	402	10	0.90
49	90.05.24 11:30	HSK,NKC	Libochovany	11900	2545	6	0.97
50	90.05.25 10:27	HSK,NKC	Merkur	2887	208	14	1.23
51	90.06.08 09:28	HSK	Gorkij	10039	480	22	0.82
52	90.06.08 12:46	HSK	Vršany	820	82	10	0.48
53	90.06.12 09:20	HSK	Gorkij	1279	181	12	0.36

Table VI. Quarry blasts (continued)

	time (UTC) y m d h m	station	quarry	total charge [kg]	max. charge per subexp. [kg]	number of subexp-losions	M_L HSK
54	90.06.13 08:57	HSK	Merkur	5880	363	19	0.68
55	90.06.27 09:15	HSK	VČSA	453	301	4	1.35
56	90.07.11 08:51	HSK	Gorkij	2085	170	12	0.92
57	90.07.19 08:16	HSK	Všechlapy	1776	595	3	0.39
58	90.07.27 07:21	HSK, NKC	Dobkovičky	14650	3792	4	1.37
59	90.07.31 08:23	HSK	Merkur	2556	161	19	0.59
60	90.08.14 08:01	HSK, NKC	Mikulovice	5250	2670	2	1.66
61	90.08.26 09:47	HSK	VČSA	6923	602	15	1.77
62	90.09.13 11:31	HSK	Dolánky	4205	522	8	0.81
63	90.10.02 14:59	HSK, NKC	Měrunice	15330	2791	9	1.14
64	90.10.25 08:43	HSK, NKC	Dobkovičky	21640	4692	5	1.72
65	90.10.31 11:58	HSK, NKC	Šverma	909	303	3	1.40
66	90.10.31 12:06	HSK, NKC	Vintířov	2750	275	10	0.96
67	90.11.10 10:37	HSK	Šverma	1595	399	4	1.02
68	90.12.19 12:05	HSK	Vintířov	3973	493	11	1.24
69	91.01.15 11:46	HSK, KRI PYS, JEZ	VČSA	4513	275	17	1.40
70	91.01.30 10:00	HSK	Měrunice	10000	2371	–	0.84
71	91.02.01 10:47	HSK, KRI PYS, JEZ	Šverma	728	243	3	1.04
72	91.05.20 11:03	HSK, NKC	Vintířov	3575	325	11	1.00

Table VII. Seismic stations

seismic station	coordinates		
	ϕ [°]	λ [°]	H [m]
Hora sv. Kateřiny (HSK)	50.603	13.426	584
Křížatky (KRI)	50.601	13.552	512
Pyšná (PYS)	50.539	13.436	680
Liniště (LIN)	50.583	13.502	716
Jezerka (JEZ)	50.541	13.484	359
Nový Kostel (NKC)	50.233	12.448	564

4. THE METHOD

The component product $v_R \cdot v_Z$ was used as an operator for wave type discrimination (Plešinger et al., 1986). For azimuth determination the seismogram vector $\vec{s}$ is transformed to a vector $\vec{v}$ in rotated analysis system

$$\begin{pmatrix} v_R \\ v_Z \\ v_T \end{pmatrix} = \begin{pmatrix} 0 & -\sin a & -\cos a \\ 1 & 0 & 0 \\ 0 & -\cos a & \sin a \end{pmatrix} \begin{pmatrix} s_Z \\ s_E \\ s_N \end{pmatrix} \tag{5}$$

where v_R and v_T are the radial and transverse components in the horizontal plane and v_Z is the vertical component of the seismogram vector $\vec{v}$ in the rotated analysis system, a is the back-azimuth of the v_R axis. The product $v_R.v_Z$ can be used as an operator for wave type discrimination because it is:

- positive for P waves
- negative for SV waves
- zero for SH and Love waves
- oscillates between positive and negative values with frequency 2ω for sinusoidal Rayleigh waves of frequency ω.

An example of determination of P and S waves for quarry blast using the product $v_R.v_Z$ is shown on Fig.4. The S waves are very clear in this case. The azimuth of events was determined by projection of P wave to the horizontal plane (Fig.5). The apparent incidence angle of P waves was determined by the projection of components v_R, v_Z. S-P time, ratios of maximum amplitudes A_S/A_P, A_L/A_S determined from total vectors, ratios of maximum values of the amplitude spectra S_S/S_P, S_L/S_S (Červený, 1976), predominant frequencies f_P, f_S, f_L, azimuth and apparent incidence angle were picked from seismograms. The picking of S waves was in many cases complicated.

The time-independent spectral modulation was studied by use of frequency-time displays known as sonograms (Hedlin et al., 1989). Amplitude spectrum was computed from the vertical component within the time interval 1s and the shift 100 points (Fig.6). Computed matrix of three values (time, frequency, spectral amplitude) was processed by the program SURFER. Fig.7 and Fig.8 show two types of sonograms: the surface and topography of the surface. The topography is convenient for complicated sonograms.

5. RESULTS

Characteristic values determined by the analysis of seismograms are summarized in Figs.9-19. The graphs can help us to find characteristic features that would be utilized for seismic discrimination between earthquakes and explosion sources. Fig.9 shows dependence between ratios of maximum amplitudes S/P and L/S waves.

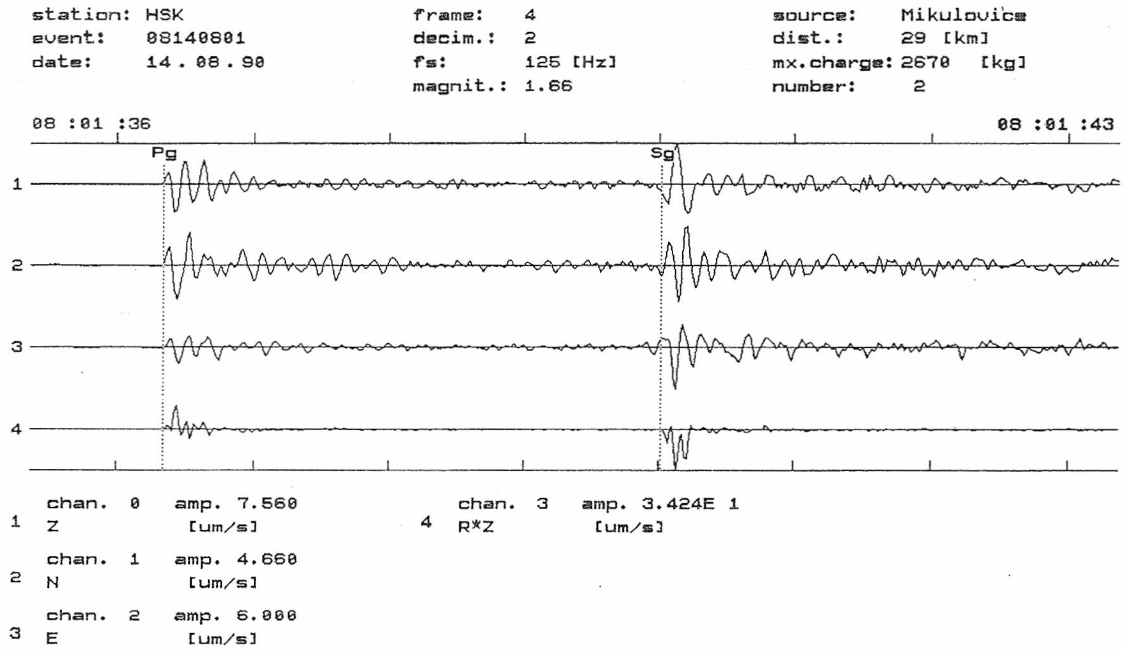

Fig. 4. The component product $v_R . v_Z$ can be used for the wave type discrimination.

A group of earthquakes is characterized by strong S waves and some of quarry blasts show strong surface (L) waves. But a great amount of events cannot be distinguished using this criteria. Fig.10 shows dependence between ratios of maximum values of amplitude spectra S/P and L/S and the results are similar as given in the previous Figure 9. Fig.11 represents dependence between epicentral distance and apparent incidence angle. The small angles are typical for earthquakes and refraction explosions at small epicentral distances. Fig.12 reveals that earthquakes and refraction explosions are characterized by high frequencies of P waves at small epicentral distances. The dependence of frequency of S waves and epicentral distance was not observed (Fig.13). A lot of earthquakes and refraction explosions have no surface (L) waves (Fig.14). The predominant frequency of P, S and L waves decreases with increasing maximum charge (Figs.15-17). Dependence between ratios of maximum amplitudes S/P, L/S waves, ratios of maximum values of amplitude spectra S/P, L/S waves and maximum charge was tested. While the dependence for ratios S/P waves was not found the ratios for L/S waves show, that great charges produce weak L waves (Figs.18-19).

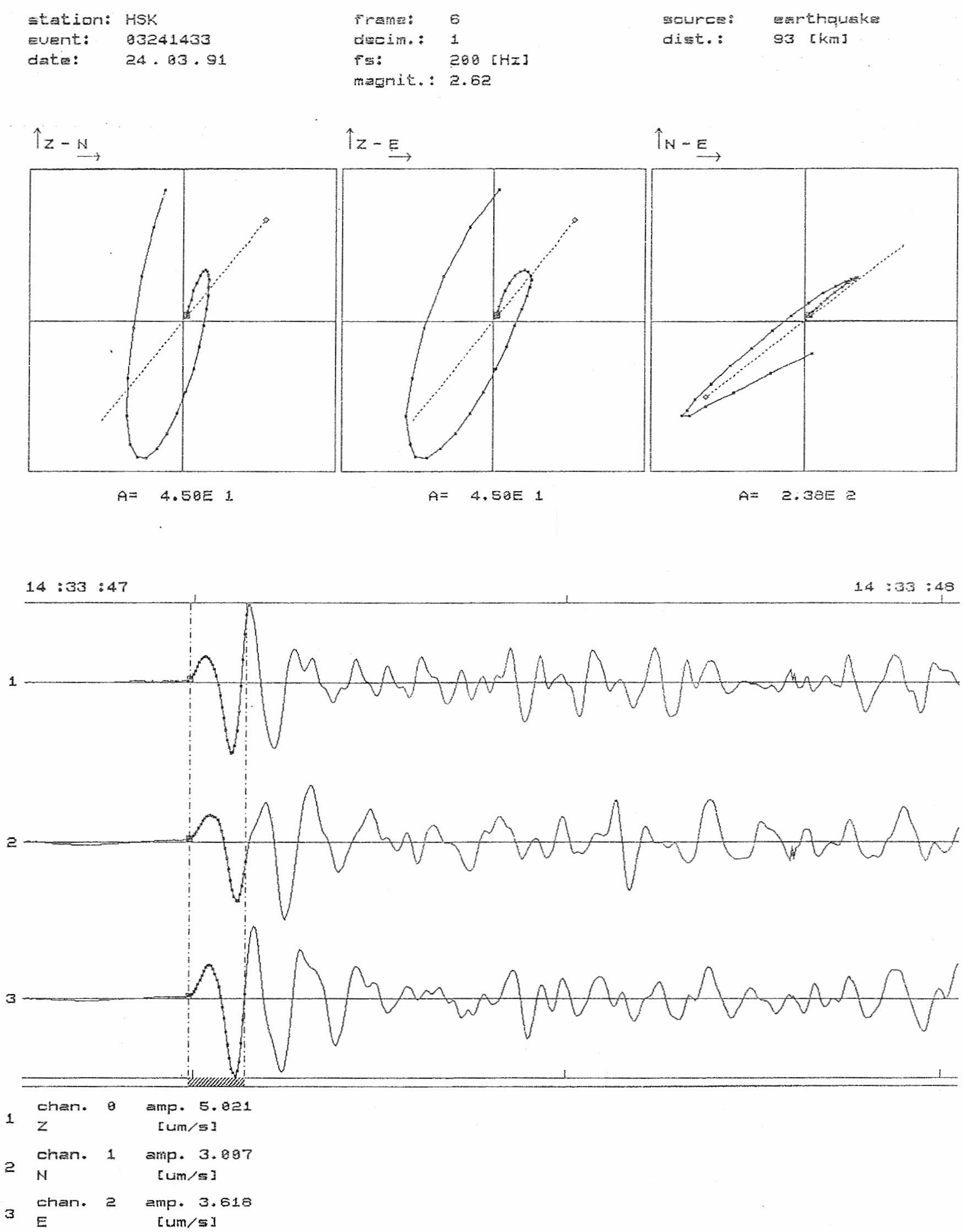

Fig. 5. Determination of the azimuth.

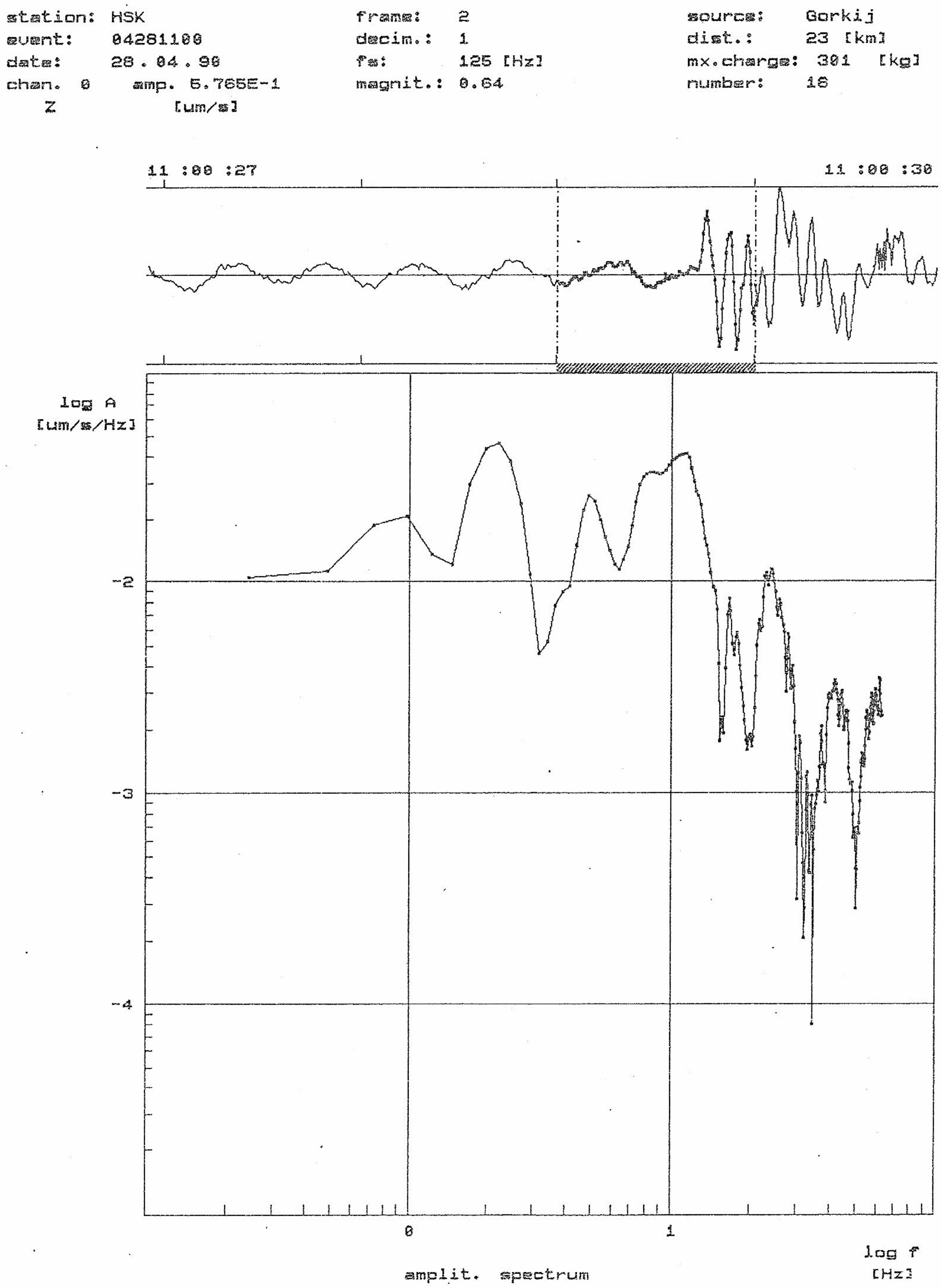

Fig. 6. Amplitude spectrum computed for 1s of the Z component.

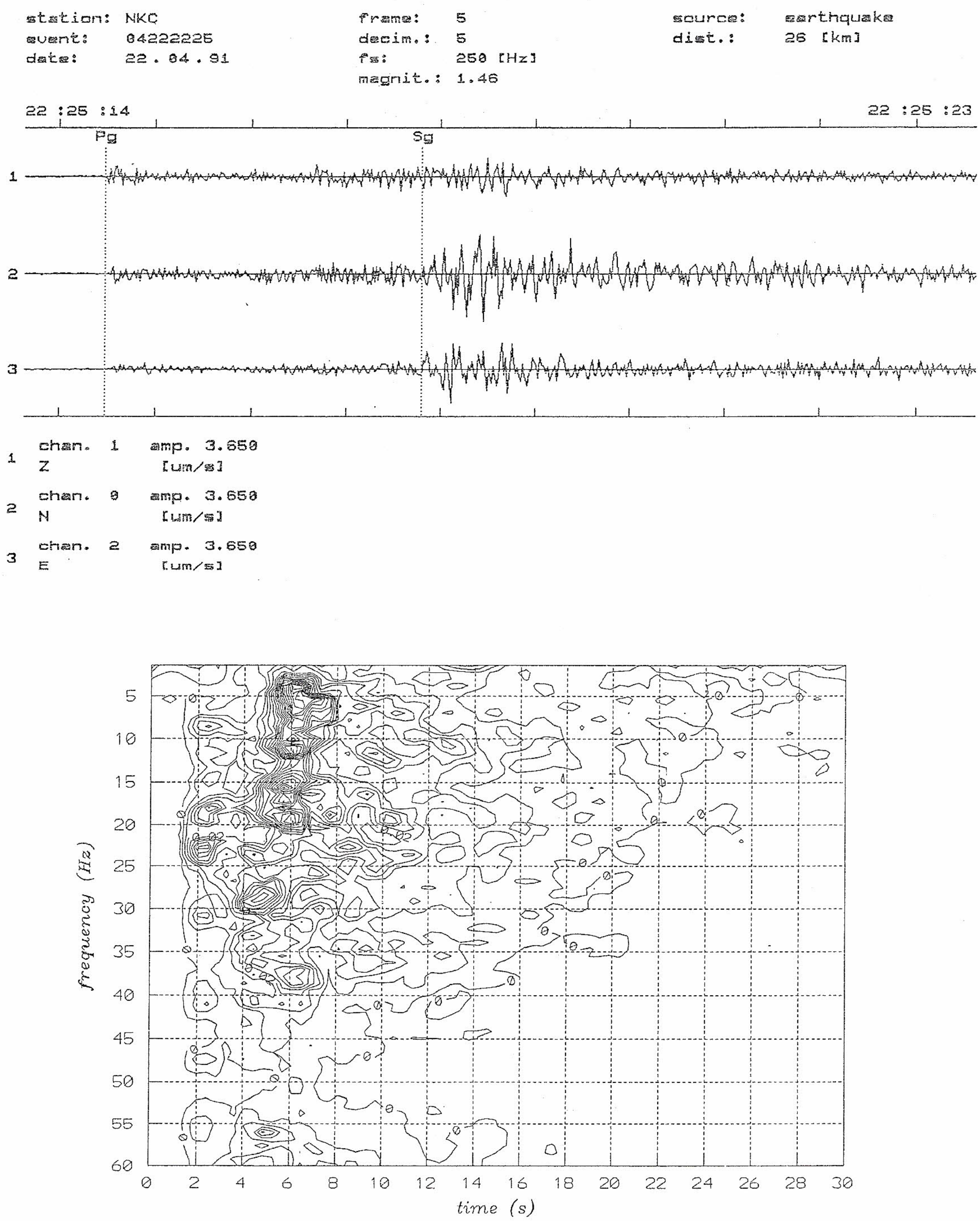

Fig.7. Seismogram and topography of the sonogram for an earthquake in Western Bohemia.

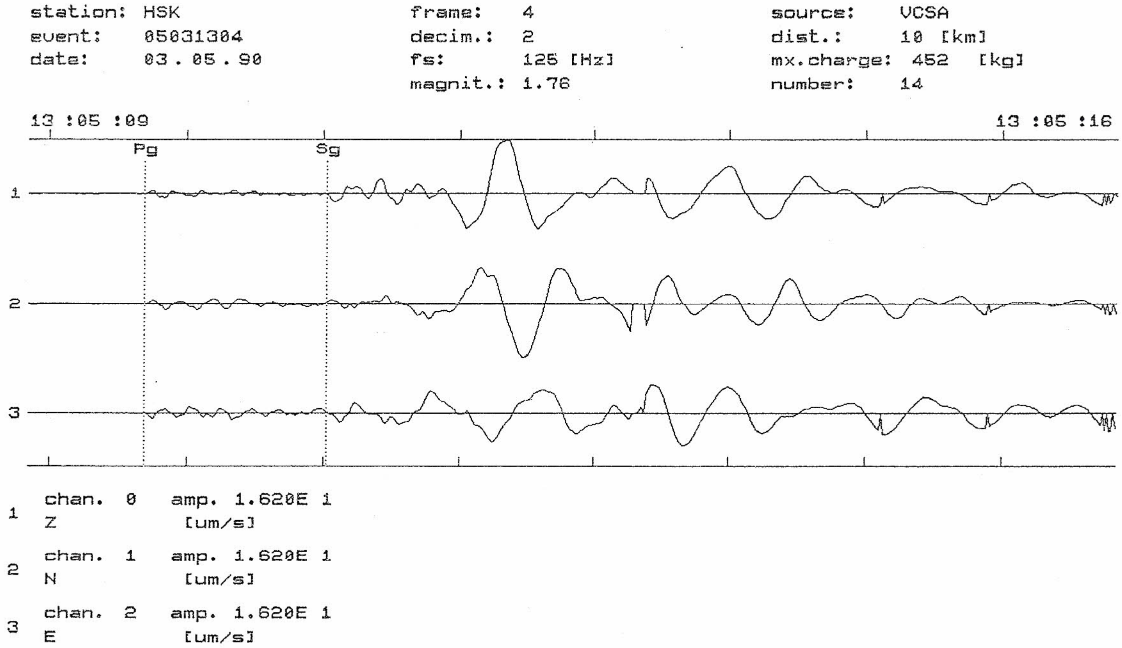

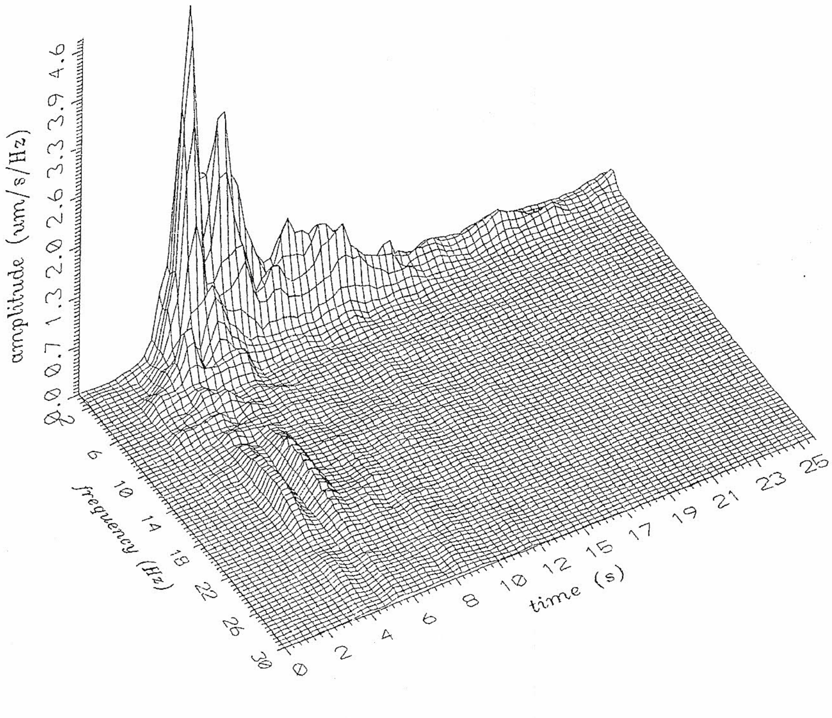

Fig.8. Seismogram and surface of the sonogram for a quarry blast in the quarry VČSA.

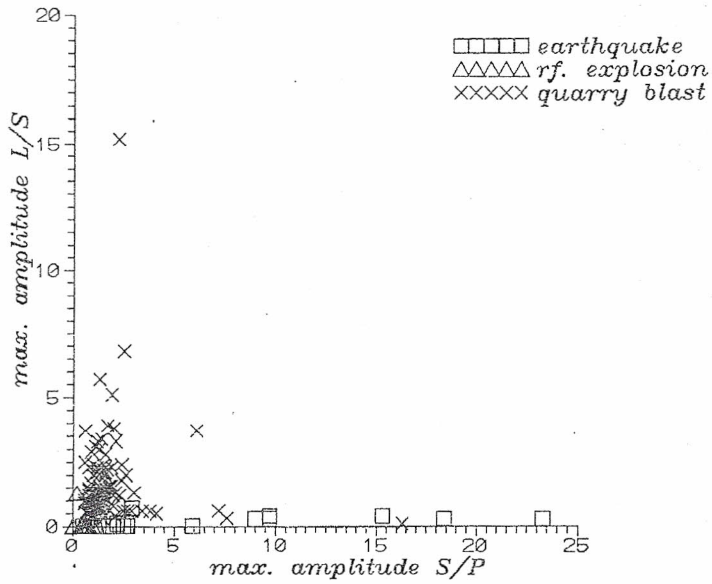

Fig. 9. Dependence between the ratios of maximum amplitudes of S/P and L/S waves.

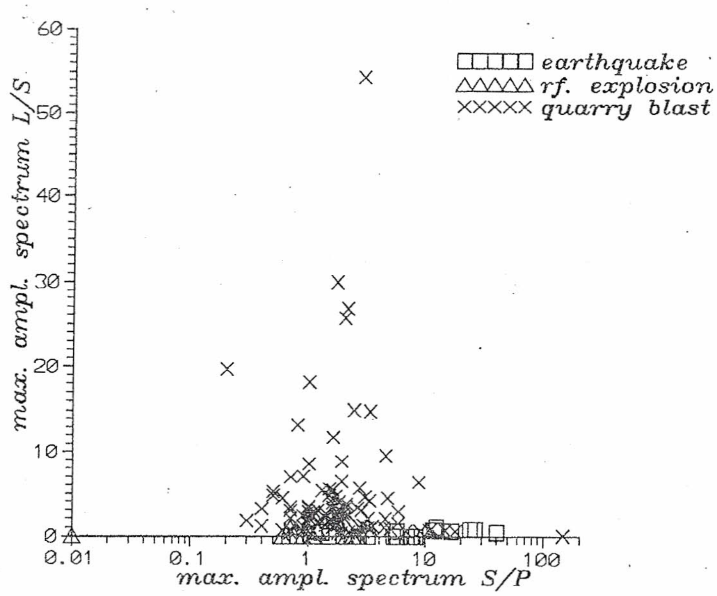

Fig.10. Dependence between the ratios of the amplitude spectrum maxima of S/P and L/S waves.

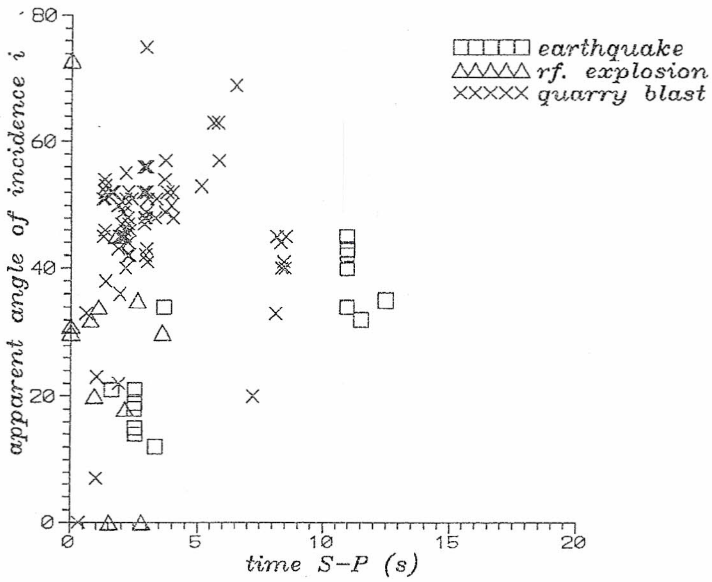

Fig. 11. Dependence between the time S-P and apparent angle of incidence i.

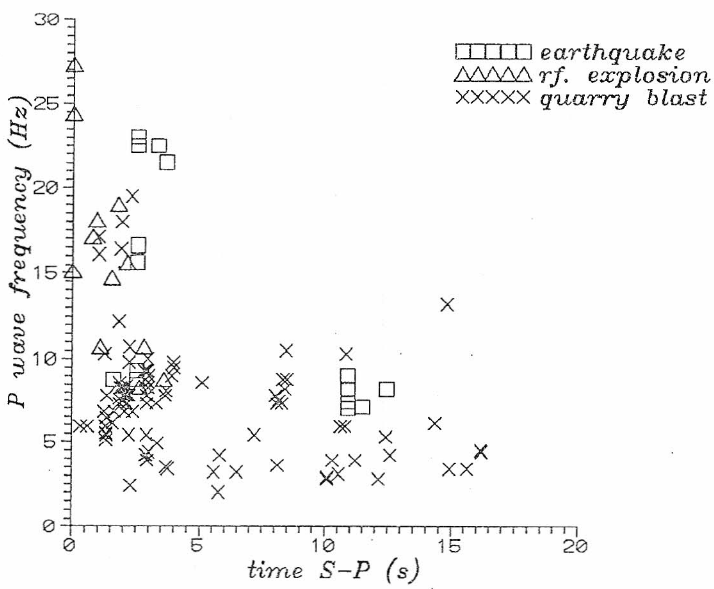

Fig. 12. Dependence between the time S-P and P wave frequency.

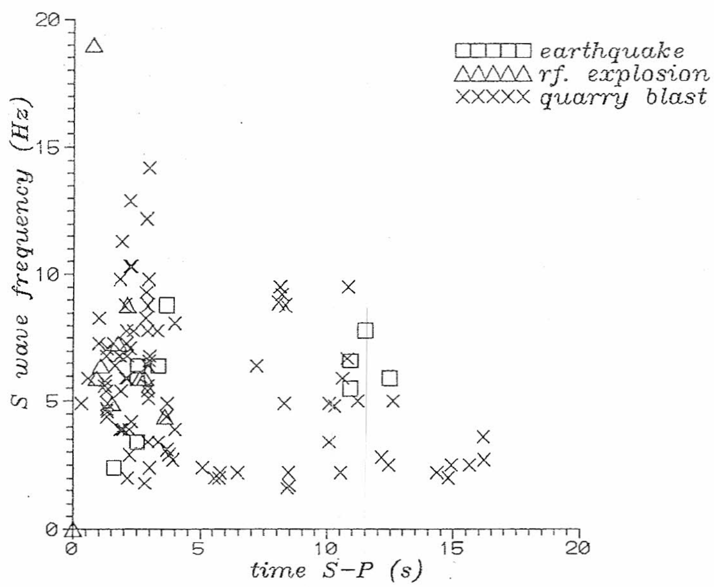

Fig. 13. Dependence between the time S-P and S wave frequency.

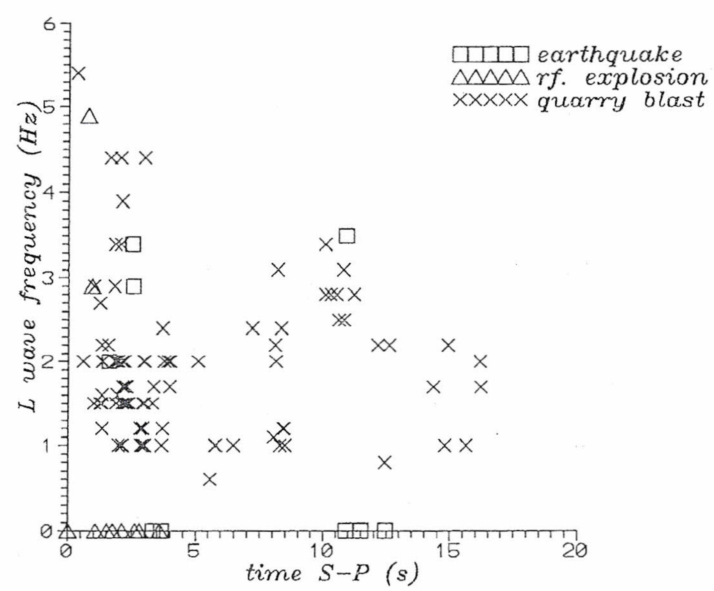

Fig. 14. Dependence between the time S-P and L wave frequency.

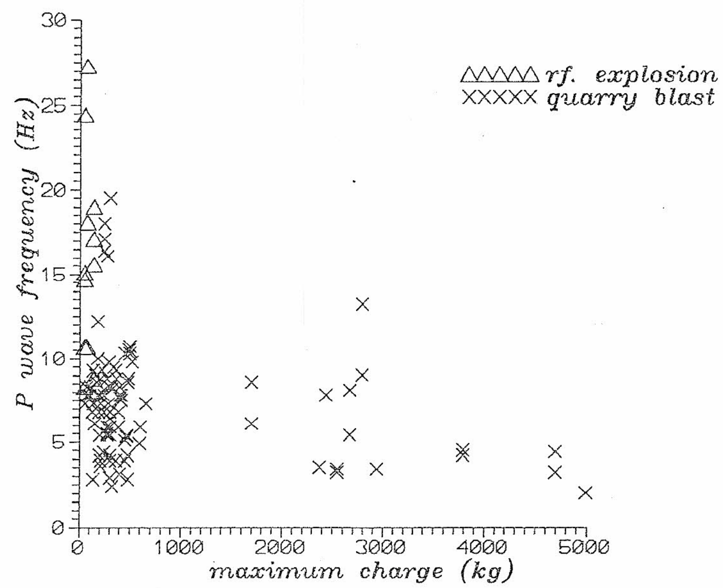

Fig.15. Dependence between maximum charge and P wave frequency.

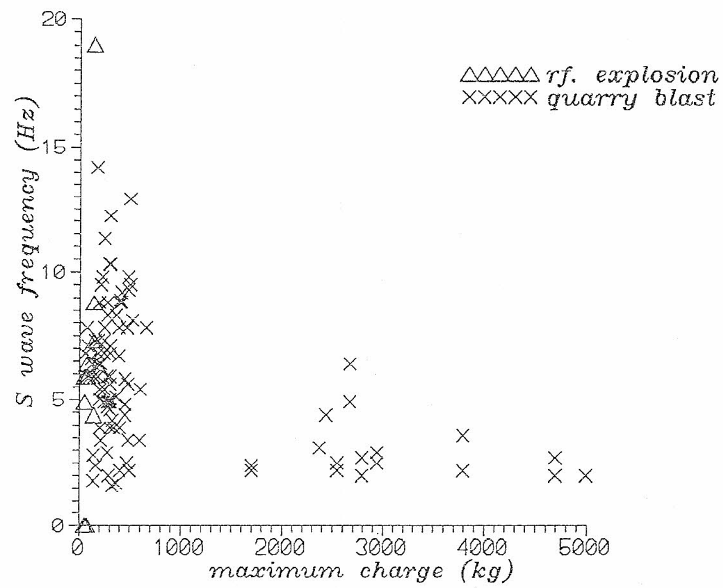

Fig.16. Dependence between maximum charge and S wave frequency.

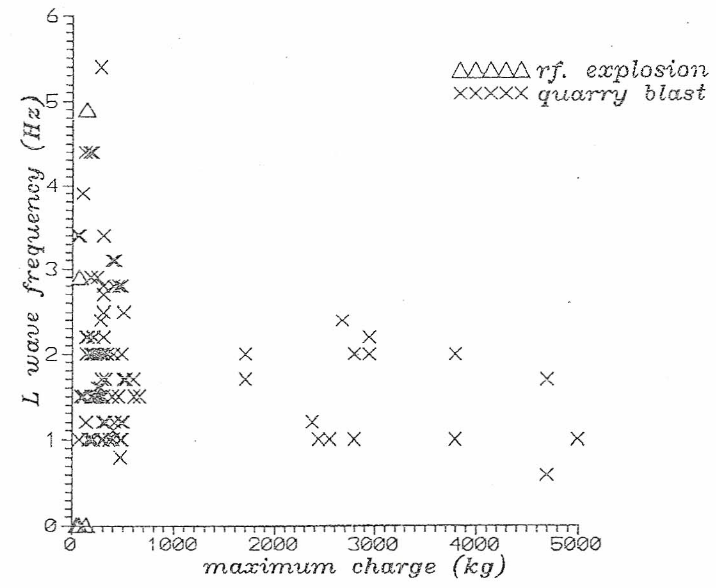

Fig.17. Dependence between maximum charge and L wave frequency.

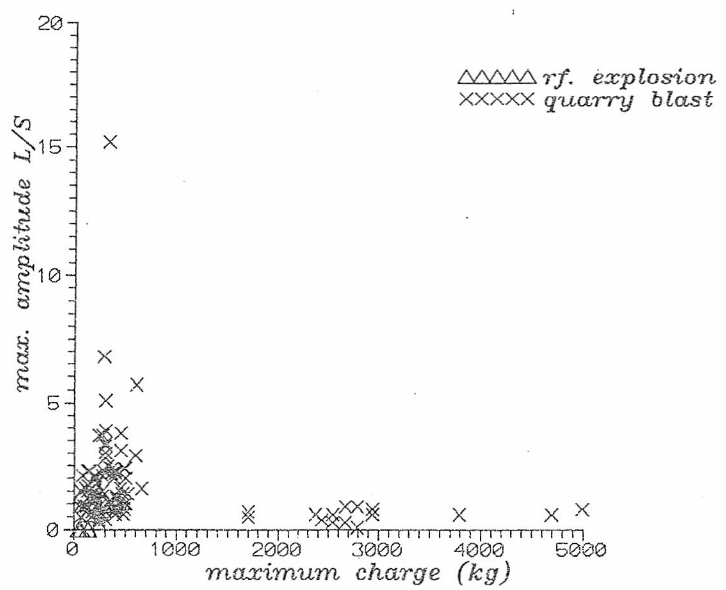

Fig.18. Dependence between maximum charge and ratio of maximum amplitudes of L/S waves.

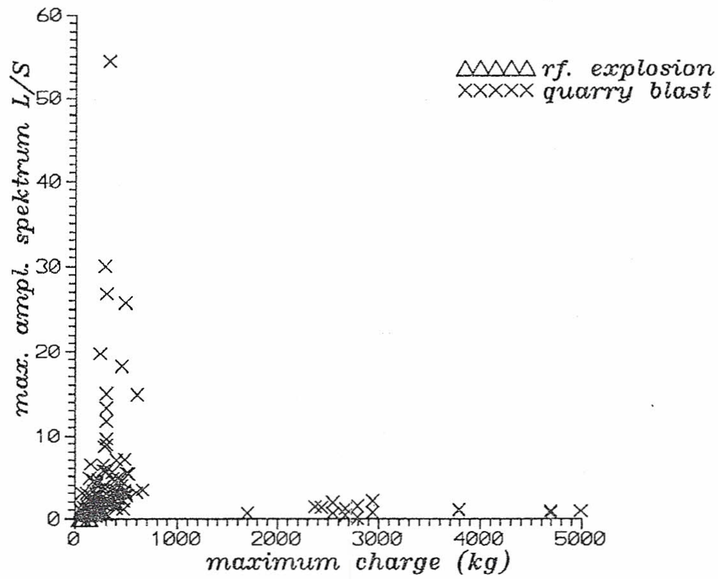

Fig.19. Dependence between maximum charge and ratio of amplitude spectrum maxima of L/S waves.

6. DISCUSSION

Verification of theoretical conclusions dealing with differences between earthquakes and explosion sources was tested on 17 seismograms of earthquakes, 12 seismograms of refraction explosions and 108 seismograms of quarry blasts from 15 various quarries in the area of North Western Bohemia. Following conclusions from the discussion of criteria in chapter 2 were achieved:

1. The first P wave arrival has been positive (compression) for all explosion sources. The difficulties are caused by the bad signal to noise ratio.

2. There is a lot of explosion sources with strong S waves with amplitude equal or greater than P waves for small and great epicentral distances.

3. Many earthquakes and refraction explosions generate weak or no surface waves. However, some quarry blasts show weak surface waves.

4. Predominant frequencies of earthquakes and refraction explosions for P waves are higher than for quarry blasts. The dimension of earthquake source should be much greater than explosion source so the frequencies would be lower for earthquakes. There are no differences in predominant frequencies for S waves. Surface waves are usually lacking in earthquakes and refraction explosions.

5. Computed sonograms for quarry blasts have shown, that there are no frequency modulations independent on time. This can be explained by the fact, that delays between explosions are irregular and the signals cannot interfere or the time independent modulation is attenuated by media. Time dependent frequency modulations for each type of wave for many events (earthquakes, refraction explosions, quarry blasts) were observed. These modulations can be explained by reflections on geological structures.

6. A lot of sonograms of quarry blasts have shown a lack of energy in high frequencies as compared to earthquakes.

We can say, that unambiguous criteria for discrimination of earthquakes, refraction explosions and quarry blasts in North Western Bohemia were not found. Thus the use of automatic methods for discrimination is not clear in this region. In the case of existence of reliable criteria the difficulty is in the automatic picking of input parameters. The automatic methods are suitable for picking first arrivals of P waves (good signal to noise ratio is supposed), but there are great problems when these methods are used for other phases. So, when it is necessary to pick the parameters manually, the experienced operator is more reliable than automatic methods. An important task for the future would be to solve problems enabling reliable location of seismic events based on 3-D P wave velocity model.

REFERENCES

Aki,K., P.G.Richards (1980). Quantitative seismology, theory and methods. W.H.Freeman, San Francisco (Russian translation Mir, Moscow 1983).

Bucha,V., T.Jíra (1992). Seismic observations in the North Bohemian coal area, Publ. Inst. Geophys. Pol. Acad. Sci., M-16 (245), 189-202.

Červený,V. (1976). Simple procedures for Fourier and Hilbert transformation. In: Proceedings of Theory and computers in geophysics, vol.5, Loučná 1975, 178-187, in Czech.

Deneva,D., L.Christoskov, B.Babachkova, N.Dotzev, K.Marinova (1988). On the discrimination between industrial explosions and weak earthquakes using records of local seismic networks, Induced seismicity and associated phenomena, Geophysical Institute, Czechosl.Acad.Sci.,Praha.

Dysart,P.S., J.J.Pulli (1990). Regional seismic event classification at the NORESS array: Seismological measurements and the use of trained neural networks. Bull.Seism.Soc.Am.80, 1910-1933.

Hedlin,M.A.H., J.B.Minster,and J.A.Orcutt (1989). The time-frequency characteristics of quarry blasts and calibration explosions recorded in Kazakhstan, U.S.S.R., Geophys.J.99, 109-121.

Hedlin,M.A.H., J.B.Minster,and J.A.Orcutt (1990). An automatic means to discriminate between earthquakes and quarry blasts, Bull.Seism.Soc.Am.80, 2143-2160.

Hussein,I.A.(1989). Seismic discrimination between natural earthquakes and industrial explosions, Ph.D. thesis, Faculty of Mathematics and Physics, Charles University of Prague.

Plešinger,A., M.Hellweg, D. Seidl (1986). Interactive high-resolution polarization analysis of broad-band seismograms, J.Geophys.59, 129-139.

Sharpe,J.A.(1942). The production of elastic waves by explosion pressures,I, Theory and empirical field observations, Geophysics 7, 144-154.

Smith,A.T.(1989). High-frequency seismic observations and models of chemical explosions: implications for the discrimination of ripple-fired mining blasts, Bull.Seism.Soc.Am.79, 1089-1110.

Su,F., K.Aki, N.N.Biswas (1991). Discriminating quarry blasts from earthquakes using coda waves, Bull.Seism.Soc.Am.81, 162-178.